

**One-dimensional miniband formation in closely stacked InAs/GaAs quantum dots**

Akihiro Takahashi, Tatsuya Ueda, Yusuke Bessho, Yukihiro Harada, and Takashi Kita

*Department of Electrical and Electronic Engineering, Graduate School of Engineering, Kobe University, 1-1 Rokkodai, Nada, Kobe 657-8501, Japan*

Eiji Taguchi and Hidehiro Yasuda

*Research Center for Ultra-High Voltage Electron Microscopy, Osaka University, 7-1 Mihogaoka, Ibaraki, Osaka 567-0047, Japan*

(Received 31 January 2013; revised manuscript received 9 May 2013; published 27 June 2013)

We have studied the electronic states of closely stacked InAs/GaAs quantum dots (QDs) with a 4.0-nm spacer layer using linearly polarized photoluminescence (PL) and time-resolved PL measurements. An increase in the stacking-layer number (SLN) leads to an increase in the linear polarization anisotropy in the (001) plane; the  $[-110]$ -polarization component becomes dominant. These SLN-dependent polarization characteristics result from the valence-band mixing induced by the vertically coupled electronic states. The PL spectrum of the stacked QDs shows clear blueshifts with an increase in the excitation power because of the band filling. In addition, the radiative recombination lifetime has been found to obey the  $T^{1/2}$  dependence, which directly confirms the one-dimensional translational motion of excitons in the closely stacked QDs.

DOI: [10.1103/PhysRevB.87.235323](https://doi.org/10.1103/PhysRevB.87.235323)

PACS number(s): 81.07.Ta, 81.05.Ea, 78.55.Kz, 81.15.Hi

**I. INTRODUCTION**

Self-assembled InAs/GaAs quantum dots (QDs) have attracted considerable interest because of their potential application in novel optoelectronic devices such as low-threshold, coolerless, direct modulation lasers,<sup>1,2</sup> polarization-insensitive broadband semiconductor optical amplifiers,<sup>3-7</sup> and high-conversion efficiency photovoltaics using intermediate bands in the optical gap.<sup>8</sup> Highly stacked QDs are required to make three dimensionally controlled artificial structures and to enhance the strength of optical responses in InAs/GaAs QD structures. Due to a strain field near the self-assembled InAs QDs, the InAs deposited on a thin GaAs capping layer forms QDs immediately above the bottom QDs, enabling us to form vertically stacked InAs/GaAs QD structures. Conversely, electronic coupling between the QDs is essential to control the optical selection rule<sup>9,10</sup> and miniband formation.<sup>11,12</sup> Various types of QD structures, such as strain-controlled InAs/GaAs QDs,<sup>5</sup> columnar InAs/GaAs and InAs/InGaAsP QDs,<sup>4,13-15</sup> and closely stacked InAs/GaAs and InAs/InGaAlAs QDs,<sup>7,16-19</sup> have been proposed to control electronic states.

Closely stacked QDs have a moderately thick spacer layer between the QD layers. The coupling strength between the electronic states in vertically stacked QDs can be controlled by changing the spacer layer thickness.<sup>20</sup> Such vertically coupled QDs lead to the formation of effective electronic states similar to the columnar QDs. In addition, the total number of QD layers used in closely stacked QDs that achieve a similar optical polarization feature is less than the number in columnar QDs.<sup>7</sup> Highly stacked QDs generally cause a change in the lateral QD size with the stacking and tend to generate dislocations.<sup>21,22</sup> A strain compensation growth technique was proposed to reduce the dislocation formation. In this technique, accumulation of the lattice-mismatched strain could be compensated for by utilizing some oppositely strained materials against the substrate.<sup>23-25</sup>

We recently demonstrated a continuous control of the linear polarization anisotropy in closely stacked InAs/GaAs

QDs by changing the stacking-layer number (SLN) without the use of the strain compensation technique.<sup>7,18</sup> In this method, the GaAs spacer layer thicknesses were less than 5 nm, which is expected to be sufficiently thin to form the miniband. Conversely, the critical thickness of InAs, showing self-assembled QD formation in the stacked layers, becomes smaller than the thickness of the first layer, which occurs for GaAs spacer layers thinner than  $\sim 20$  nm.<sup>26</sup> Therefore, controlling the InAs nominal thicknesses in the stacked layers will enable us to reduce the excess strain accumulation in highly stacked InAs/GaAs QDs.<sup>7</sup> In the present study, we fabricated highly stacked InAs/GaAs QDs with a 4.0-nm GaAs spacer layer by reducing the thickness of InAs in the stacked layers. Detailed photoluminescence (PL) properties of the stacked QD, as a function of the SLN, have been investigated. Linear polarization properties, excitation power dependence, and the radiative recombination lifetime clearly confirm the one-dimensional (1D) miniband formation in the stacked InAs/GaAs QDs.

**II. QD GROWTH AND EXPERIMENTAL DETAILS**

The InAs QDs were grown on undoped GaAs(001) substrates by solid-source molecular beam epitaxy. After a thermal cleaning of the substrate at 570 °C under As<sub>2</sub> at a pressure of  $1.3 \times 10^{-3}$  Pa, a 400-nm-thick GaAs buffer layer was grown at 550 °C. The InAs QD layers were formed by self-assembly on the buffer layer. For the growth of the InAs QDs, the substrate surface temperature, monitored using an infrared pyrometer, was lowered to 480 °C. The nominal thickness of the deposited InAs was 2.0 monolayers (MLs) for the first QD layer. A 4.0-nm-thick GaAs spacer layer was deposited on it. A growth interruption of 10 s was introduced after growing the GaAs spacer layer, following which subsequent InAs QD layers with a reduced thickness of 1.4 MLs were alternatively formed on the GaAs spacer layer. The SLNs of the InAs/GaAs QDs used in this study were 1, 9, 15, 20, and 30. Finally, a 100-nm-thick GaAs capping layer was deposited.

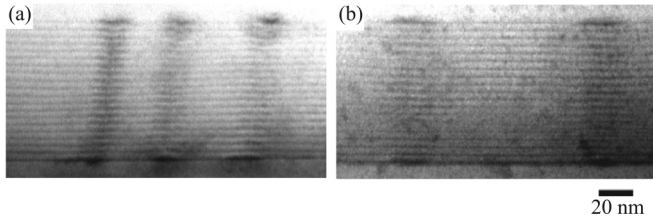


FIG. 1. (a)  $(-110)$  and (b)  $(110)$  cross-sectional TEM images of the 20 stacked InAs QDs.

Continuous-wave PL measurements were carried out by using two laser diodes with wavelengths 659 and 532 nm. The PL signal was dispersed using a 30-cm single monochromator and detected by a liquid-nitrogen-cooled InGaAs-diode array. We carefully studied the temperature dependence of the radiative recombination lifetime using a near infrared streak camera system having a temporal resolution of 20 ps. The light source used was a mode-locked Ti:sapphire pulse laser with a pulse width of approximately 130 fs and a repetition rate of 4 MHz. The excitation wavelength and excitation power density were 800 nm and  $1.5 \text{ nJ/cm}^2$ , respectively. The surface morphology of the InAs QDs without a capping layer was characterized by using an atomic force microscope, and the crystallographic properties of the stacked QDs were examined by using a cross-sectional transmission electron microscope (TEM). The QD density was approximately  $1.0 \times 10^{10} \text{ cm}^{-2}$ . Typical cross-sectional TEM images of the stacked QDs observed from the  $[110]$  and  $[-110]$  directions are shown in Fig. 1. The SLN used in the TEM observation was 20. The wetting-layer interfaces were very clear, and the well-aligned stacking of the QDs was confirmed. The stacking direction was found to tilt slightly toward the  $[110]$  direction in the  $(-110)$  cross section. Such tilting was not obvious in the  $(110)$  cross section. This anisotropic tilting behavior of the stacked QDs is considered to be caused by an anisotropic migration of In atoms on the  $(001)$  growth front.<sup>27</sup>

### III. EXPERIMENTAL RESULTS AND DISCUSSION

#### A. Linearly polarized PL and the origin of PL signals

Figure 2 shows the linearly polarized PL spectra of the stacked InAs QDs with different SLNs at room temperature. A laser diode with the wavelength of 659 nm was used for the excitation. The excitation power was  $94 \text{ W/cm}^2$ . Figures 2(a) and 2(b) display the PL spectra obtained from the  $(-110)$ -cleaved surface and the  $(001)$  surface, respectively. The  $[001]$ -polarization component (red line) along the stacking direction is greatly enhanced as the SLN increases, as shown in Fig. 2(a). This is direct evidence of electronic coupling along the stacking direction.<sup>7,16</sup> Conversely, as shown in Fig. 2(b), the polarized PL in the  $(001)$  plane also shows a dramatic change in the polarized PL; the  $[-110]$ -polarization component (green line) becomes dominant with an increase in the SLN. The single-layer QD does not show such in-plane anisotropy. Yu *et al.* have reported similar phenomena in stacked InGaAs/GaAs QDs.<sup>28</sup> According to our recent theoretical calculations,<sup>10,18</sup> the key mechanism creating a dramatic change in the linear polarization properties as a function of the SLN has been made clear that it is attributed

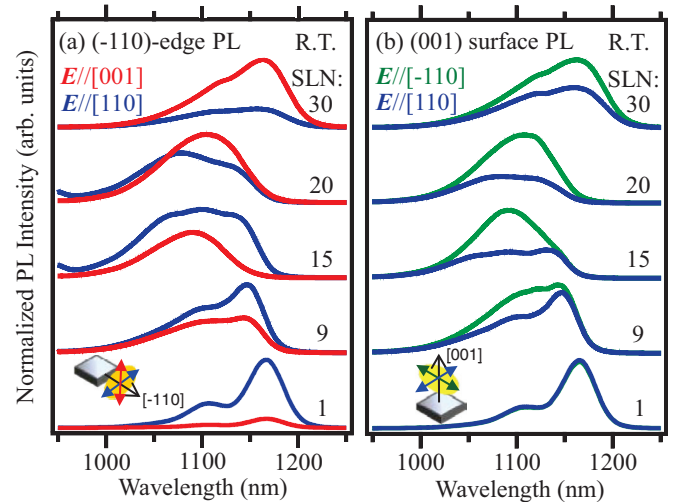


FIG. 2. (Color online) Linearly polarized PL spectra from the (a)  $(-110)$ -cleaved surface and (b)  $(001)$  surface.

to the valence-band mixing. In case the vertical height along the  $[001]$  direction is sufficiently smaller than the lateral size in the  $(001)$  plane, the fundamental valence-band state in QDs consists of the heavy-hole component, which is very easy to understand if we image electronic states in quantum wells. This diminishes the in-plane polarization anisotropy. As the QD height increases along the  $[001]$  direction, the  $[001]$ -polarization component increases drastically, and the in-plane polarization anisotropy becomes significant according to the in-plane shape anisotropy and/or piezoelectricity. The relatively strong in-plane quantum confinement induces heavy- and light-hole mixing. Such electronic states are similar to those in quantum wires. Detailed experimental and atomistic theoretical studies of degree of polarization from stacked QDs have been discussed in Ref. 10.

The 9 and 15 stacked QDs show several peaks in the PL spectrum. To clarify the origins of these PL signals, we measured the PL at 16 K. The 659-nm wavelength laser diode was used for the excitation, and the excitation power was  $3.2 \text{ W/cm}^2$ . Figure 3(a) shows the unpolarized PL spectra observed from the  $(001)$  surface. The PL spectra of the 9- and 15-layer stacked QDs consist of two peaks labeled A and B, as indicated by the arrows. Figure 3(b) shows the in-plane PL linear polarization properties of the same samples. While peak A exhibits a remarkable anisotropy, PL peak B is isotropic. This result indicates that peak B represents a signal obtained from the isolated QDs that fails to couple along the growth direction. Conversely, the anisotropy of peak A is caused by valence-band mixing, and therefore, this signal is obtained from the electronically coupled QDs along the growth direction. To verify these assignments, we measured the PL with different excitation wavelengths.<sup>29</sup> The measurements have been performed by selecting the same excitation area of the sample. The difference in the penetration depth of the excitation laser light clearly distinguishes the signals whose origins distribute along the growth direction. Figure 4 shows the PL spectra excited by the 659-nm (dashed line) and 532-nm (solid line) wavelength laser diodes. The penetration depths for the 659- and 532-nm laser diodes are approximately 305 and 143 nm,

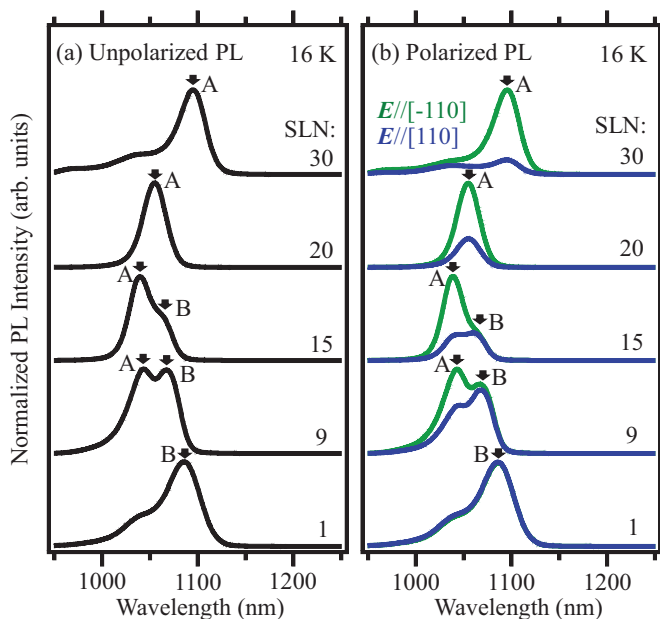


FIG. 3. (Color online) (a) Unpolarized and (b) polarized PL spectra from the (001) surface at 16 K.

respectively. The excitation power used here was  $3.2 \text{ W/cm}^2$ . The PL intensity of peak B, attributed to the isolated QDs, becomes relatively weak when the excitation wavelength is 532 nm. Thus, the penetration depth of the excitation laser light is relatively shallow. Therefore, it is concluded that the vertical coupling becomes certain by repeating the stacking. In fact, peak B of the isolated QDs becomes relatively weak with an increase in the stacking, and consequently, the PL spectra show only peak A, which is attributed to the vertically coupled QDs in the 30 stacked QDs. In this experiment, the excitation power of these different lasers was the same:  $3.2 \text{ W/cm}^2$ . Therefore,

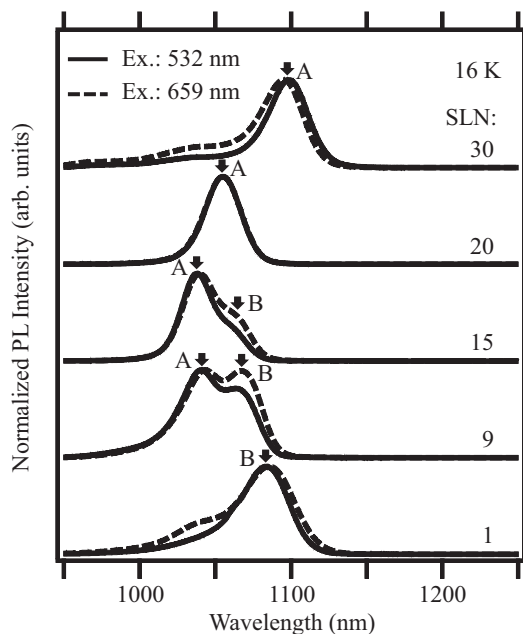


FIG. 4. PL spectra excited by 659-nm (dashed line) and 532-nm (solid line) wavelength laser diodes.

the excitation photon number of the 659-nm laser is larger than that of the 532 nm, which is considered to cause the excited emission in the spectrum of the single-layer QD (SLN = 1) in 659 nm. However, since the peak separation (50 meV) of the excited state and the fundamental state is larger than that (25 meV) between the peaks A and B, the contribution of the excited state of peak B to peak A is considered to be small.

It is noted here that the peak wavelength of peak A shows a peculiar change; with an increase in the SLN, peak A initially shifts toward the shorter wavelength side and then shows a redshift. This change is considered to be caused by the alloy mixing of In and Ga in the stacked QDs. At an earlier stage of stacking, incorporating Ga into the stacked QDs causes a blueshift. As the stacking increases, an increase in the QD volume leads to a redshift.

### B. Excitation power dependence of PL and band-filling effects

We also investigated the excitation power dependence of the PL spectrum to confirm whether the band-filling effect expected for a miniband in the closely stacked QDs. Figures 5(a)–5(e) show the excitation power dependences of the PL spectra of the single-layer, 9, 15, 20, and 30 stacked QDs, respectively. The PL spectra were measured at 16 K to avoid a spatial carrier redistribution induced by the thermal energy.<sup>30</sup> The 532-nm wavelength laser diode was used to reduce the contribution of the emission from the isolated QDs located near the bottom of the stacked QDs. The PL peak wavelength of the single-layer QDs was almost independent of the excitation power, as shown in Fig. 5(a). Conversely, the PL peaks of the stacked QDs showed a clear blueshift with an increase in the excitation power. The blueshift increased with the stacking and was measured to be 3, 4, 4, and 5 meV for the 9-, 15-, 20-, and 30-layer-stacked QDs, respectively. Sugaya *et al.*<sup>31</sup> has stated that the miniband width induces a blueshift in the PL peak wavelength as the excitation power density is increased. With the blueshift in a stacked QD (single quantum wire), it is very difficult to understand that validity because of its extremely peaked density of state. Nevertheless, the blueshift can occur, if we assume that the electronic states are not perfectly uniform and are slightly distributed along the stacking direction. The populated carriers in the dispersed states below the quasi-Fermi level under the light illumination are able to transfer to spatially adjacent states. This causes a blueshift. Therefore, the blueshift is not direct evidence reflecting the miniband formation although the populated carriers in the “dispersed states” in the miniband are essential to cause the blueshift. By the way, it is necessary to state the contribution of the excited state of peak B looking like it is overlapping with peak A. As mentioned above, the peak separation of the excited state and the ground state is larger than that between peaks A and B. Moreover, peak A of the 30 stacked QDs in which peak B disappears did show a clear blueshift of 5 meV. These results suggest that the contribution of the excited state of peak B to the blueshift of peak A is small.

### C. Time-resolved PL and 1D-translational motion of excitons in stacked QDs

An observation of the 1D-translational motion of excitons is essential to confirm the 1D miniband formation in closely

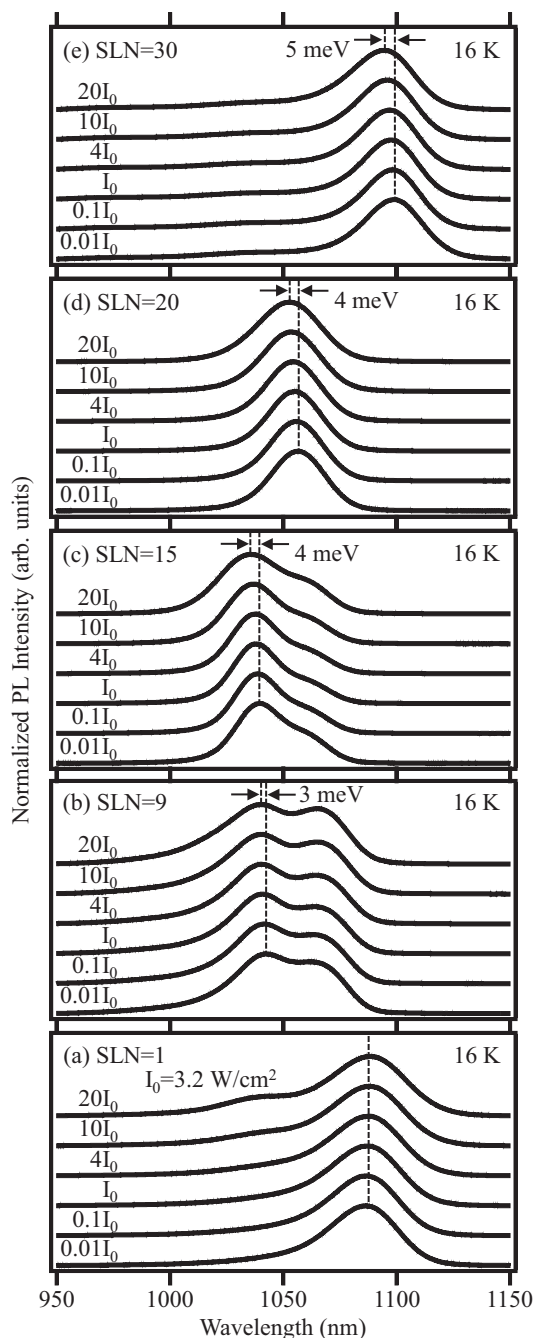


FIG. 5. Excitation power dependence of the PL spectra of the (a) single-layer, (b) 9, (c) 15, (d) 20, and (e) 30 stacked InAs QDs at 16 K.

stacked QDs. Here, we carefully measured the temperature dependence of the radiative recombination lifetime of excitons in the stacked QDs. Figure 6(a) shows the PL decay profiles for various SLNs measured at 3.1 K. The PL decay profiles of the stacked QDs were recorded within  $\lambda_0 \pm 1$  nm, where  $\lambda_0$  is the PL peak wavelength of the signal A, attributed to the stacked QDs. The PL decay profile of the single-layer QDs was recorded at the center wavelength of peak B. The decay of these QDs exhibits a simple single exponential profile. Figure 6(b) shows the PL decay lifetime calculated by fitting the temporal evolution of the PL intensity with a

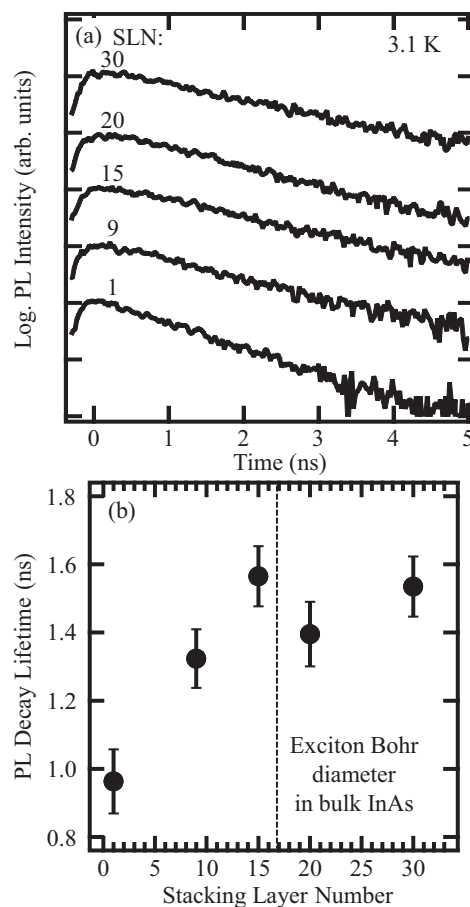


FIG. 6. (a) SLN dependence of the PL decay profile at 3.1 K, which was detected at  $\lambda_0 \pm 1$  nm. (b) SLN dependence of the PL decay lifetime. The dashed line shows the exciton Bohr diameter in bulk InAs.

single exponential function. The dashed line shows the exciton Bohr diameter in the bulk InAs. The radiative recombination lifetime is inversely proportional to the oscillator strength of the electronic dipole transition and the overlap integral of the electron and the hole-wave functions. Bellessa *et al.*<sup>32</sup> reported that the radiative lifetime decreases with an increase in the QD size because of the increase in the oscillator strength. However, the radiative lifetime observed herein increases with an increase in the SLN until the SLN equals 15 and then reaches saturation, as shown in Fig. 6(b). The strength of the electronic coupling of the electrons in the closely stacked QDs is expected to be larger than that of the holes because of their effective masses. Therefore, the overlap integral of the envelope-wave functions between the electrons and the holes decreases with an increase in the SLNs, which results in an increase in the radiative lifetime. The saturation of the radiative lifetime observed in highly stacked QDs indicates that the stacked QD height is longer than the exciton Bohr diameter of 74 nm in bulk InAs.<sup>33</sup> This suggests a breakdown of the strong quantum confinement regime in the highly stacked QDs with more than 15 SLN.

Figures 7(a)–7(e) show the PL decay profiles of the single-layer, 9, 15, 20, and 30 stacked QDs, respectively, measured at different temperatures. According to the

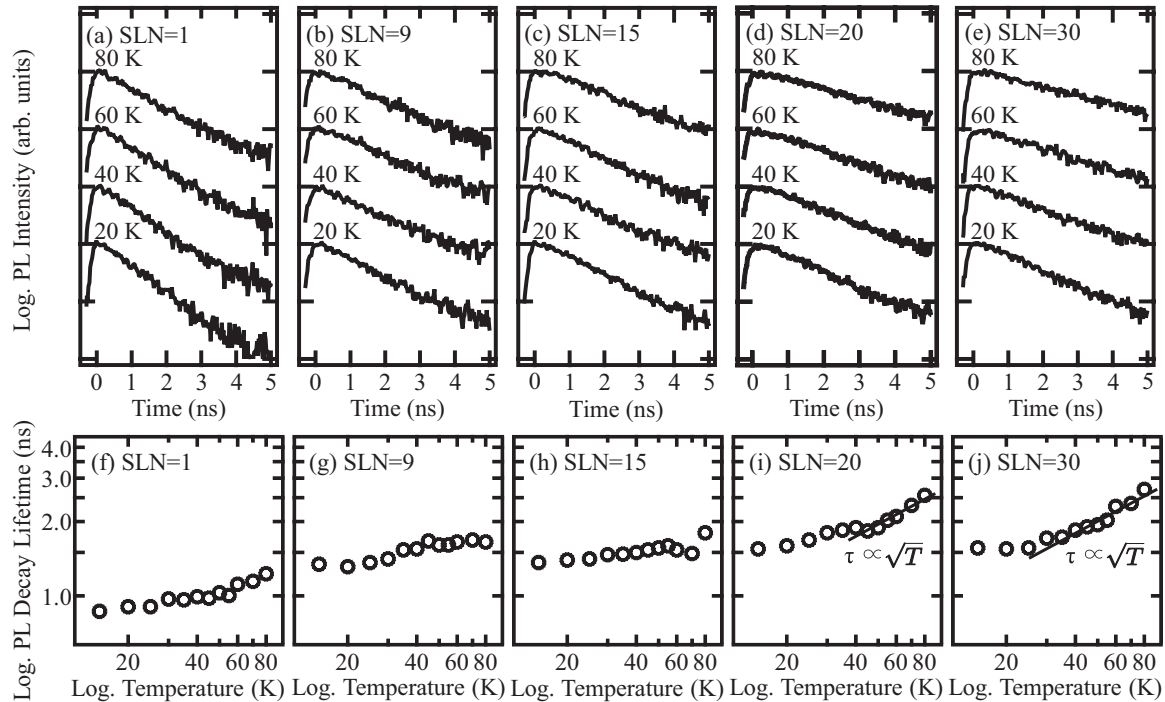


FIG. 7. Temperature dependence of the PL decay profiles of the (a) single-layer, (b) 9, (c) 15, (d) 20, and (e) 30 stacked InAs QDs, which were detected at  $\lambda_0 \pm 1$  nm. (f)–(j) Temperature dependence of the PL decay lifetime in each the sample. The solid line indicates the  $T^{1/2}$  dependence.

temperature-quenching behaviors of the integrated PL intensity for these samples, we confirmed beforehand that the radiative recombination process is dominant below 100 K. The decay shows a simple single exponential profile at all temperatures. Figures 7(f)–7(j) show the temperature dependence of the PL decay lifetimes calculated from the single exponential fitting. The change in the lifetime of the single-layer, 9, and 15 stacked QDs is small in comparison to the result of the 20 and 30 stacked QDs. A slight increase in the lifetime with the temperature observed for single-layer, 9, and 15 stacked QDs suggests a thermal delocalization of the excitons into the spacer layer and/or the upper subband levels of the electrons and the holes via thermionic emission.<sup>17</sup> In contrast, the lifetime of the 20 and 30 stacked QDs gradually increases with an increase in the temperature above 30 K and excellently obeys the  $T^{1/2}$  dependence, as depicted by the solid line. The  $T^{1/2}$  dependence of the radiative lifetime indicates the 1D translational motion of excitons<sup>34–37</sup> and therefore clearly confirms the miniband formation in the highly stacked InAs QDs. The temperature-insensitive behavior up to 30 K indicates that the hole is localized at each QD layer, and the excitons move very slightly along the growth direction at such low temperatures. In contrast to the changes in peak A, the PL decay lifetime of peak B and its temperature dependence was almost independent of the SLN.

Tomić<sup>12</sup> has reported theoretical predictions regarding the band formation in stacked InAs/GaAs QDs. According to his results, stacked QDs clearly create minibands depending on the GaAs spacer layer thickness; the 3-nm-thick GaAs spacer layer leads apparent miniband with the energy width more than 70 meV. The nominal thickness of the spacer layer used in our

stacked InAs/GaAs QDs was 4 nm, which is close to a model used in his calculations.

Generally, self-assembled QDs have a significant inhomogeneous size distribution, which leads to inhomogeneously distributed energy states. Although it has been reported in Ref. 2 that such inhomogeneity can be reduced by the stacking, energy matching demanded to create minibands seems to be very difficult. A similar question has puzzled us in case we consider laser oscillation in an inhomogeneous QD system. To interpret the lasing behavior in self-assembled InGaAs/GaAs QDs, the effect of *homogeneous* broadening of optical gain has been discussed in Sugawara *et al.*<sup>38</sup> We are considering that similar things happened in the miniband formation, that is, energy states within the homogeneous energy width can couple each other and form minibands, which relaxes the restriction demanded by the resonant energy coupling. The magnitude of the homogeneous broadening has been reported to be more than 10 meV (Ref. 38) at room temperature and extremely small, less than 0.1 meV,<sup>38,39</sup> at low temperature. The results in Fig. 7 indicate that the 1D feature clearly appear in the highly stacked QDs above  $\sim 30$  K. The appearance of the  $T^{1/2}$  dependence at such an elevated temperature seems to mean the presence of a threshold of the homogeneous linewidth achieving the electronic coupling. Since the inhomogeneously distributed energy states within the homogeneous energy width can couple and form the miniband, the energy states of QDs are considered to be moderately uniform along the stacking direction. On the other hand, the inhomogeneous PL broadening of the stacked QDs (peak A) is caused by an inhomogeneous size distribution of stacked QDs existing in the wafer plane.

#### IV. CONCLUSIONS

We have studied the miniband formation in closely stacked InAs/GaAs QDs. The in-plane polarization anisotropy as well as the [001]-polarization component increase with an increase in the SLN due to the valence-band mixing in the vertically coupled electronic states. The vertical coupling becomes certain by repeating the stacking, and the alloy mixing of In and Ga in the stacked QDs occurs. The PL spectra of the stacked QDs showed a clear blueshift with an increase in the excitation power. This is considered to be caused by a distribution of densely populated carriers in a dispersed band. The radiative lifetime increases with an increase in the SLN because of the exciton delocalization along the stacking direction. The radiative lifetime of highly stacked QDs obeys the  $T^{1/2}$  dependence. This is direct evidence of the

1D translational motion of excitons in the closely stacked QDs and confirms the formation of a dispersion relation along the stacking direction.

#### ACKNOWLEDGMENTS

This work has been partially supported by the "Nanotechnology Network Project of the Ministry of Education, Culture, Sports, Science and Technology (MEXT), Japan" at the Research Center for Ultrahigh Voltage Electron Microscopy in Osaka University, Scientific Research Grants-in-Aid from MEXT, and the European Commission and New Energy and Industrial Technology Development Organization (NEDO) through the funding of a new generation of concentrator photovoltaic cells, modules and systems (NGCPV) EUROPE-JAPAN.

- 
- <sup>1</sup>D. Bimberg, M. Grundmann, and N. N. Ledentsov, *Quantum Dot Heterostructures* (Wiley, New York, 1998), Chap. 8.
- <sup>2</sup>H. Shoji, in *Semiconductors and Semimetals*, edited by M. Sugawara, Vol. 60 (Academic, San Diego, CA, 1999), Chap. 6, pp. 241–286.
- <sup>3</sup>M. Sugawara, N. Hatori, T. Akiyama, Y. Nakata, and H. Ishikawa, *Jpn. J. Appl. Phys.* **40**, L488 (2001).
- <sup>4</sup>T. Kita, O. Wada, H. Ebe, Y. Nakata, and M. Sugawara, *Jpn. J. Appl. Phys.* **41**, L1143 (2002).
- <sup>5</sup>P. Jayavel, H. Tanaka, T. Kita, O. Wada, H. Ebe, M. Sugawara, J. Tatebayashi, Y. Arakawa, Y. Nakata, and T. Akiyama, *Appl. Phys. Lett.* **84**, 1820 (2004).
- <sup>6</sup>T. Kita, N. Tamura, O. Wada, M. Sugawara, Y. Nakata, H. Ebe, and Y. Arakawa, *Appl. Phys. Lett.* **88**, 211106 (2006).
- <sup>7</sup>T. Inoue, M. Asada, N. Yasuoka, O. Kojima, T. Kita, and O. Wada, *Appl. Phys. Lett.* **96**, 211906 (2010).
- <sup>8</sup>A. Luque, A. Martí, N. López, E. Antolín, E. Cánovas, C. Stanley, C. Farmer, and P. Díaz, *J. Appl. Phys.* **99**, 094503 (2006).
- <sup>9</sup>T. Saito, H. Ebe, Y. Arakawa, T. Kakitsuka, and M. Sugawara, *Phys. Rev. B* **77**, 195318 (2008).
- <sup>10</sup>M. Usman, T. Inoue, Y. Harada, G. Klimeck, and T. Kita, *Phys. Rev. B* **84**, 115321 (2011).
- <sup>11</sup>C. Pryor, *Phys. Rev. Lett.* **80**, 3579 (1998).
- <sup>12</sup>S. Tomić, *Phys. Rev. B* **82**, 195321 (2010).
- <sup>13</sup>P. Ridha, L. Li, A. Fiore, G. Patriarche, M. Mexis, and P. M. Smowton, *Appl. Phys. Lett.* **91**, 191123 (2007).
- <sup>14</sup>P. Podemski, G. Sęk, K. Ryczko, J. Misiewicz, S. Hein, S. Höfling, A. Forchel, and G. Patriarche, *Appl. Phys. Lett.* **93**, 171910 (2008).
- <sup>15</sup>N. Yasuoka, K. Kawaguchi, H. Ebe, T. Akiyama, M. Ekawa, S. Tanaka, K. Morito, A. Uetake, M. Sugawara, and Y. Arakawa, *Appl. Phys. Lett.* **92**, 101108 (2008).
- <sup>16</sup>O. Kojima, H. Nakatani, T. Kita, O. Wada, K. Akahane, and M. Tsuchiya, *J. Appl. Phys.* **103**, 113504 (2008).
- <sup>17</sup>O. Kojima, H. Nakatani, T. Kita, O. Wada, and K. Akahane, *J. Appl. Phys.* **107**, 073506 (2010).
- <sup>18</sup>Y. Ikeuchi, T. Inoue, M. Asada, Y. Harada, T. Kita, E. Taguchi, and H. Yasuda, *Appl. Phys. Express* **4**, 062001 (2011).
- <sup>19</sup>D. Alonso-Álvarez, J. M. Ripalda, B. Alén, J. M. Llorens, A. Rivera, and F. Briones, *Adv. Mater.* **23**, 5256 (2011).
- <sup>20</sup>D. Roy-Guay, P. J. Poole, and S. Raymond, *Semicond. Sci. Technol.* **25**, 045001 (2010).
- <sup>21</sup>Q. Xie, A. Madhukar, P. Chen, and N. P. Kobayashi, *Phys. Rev. Lett.* **75**, 2542 (1995).
- <sup>22</sup>Z. R. Wasilewski, S. Fafard, and J. P. McCaffrey, *J. Cryst. Growth* **201–202**, 1131 (1999).
- <sup>23</sup>G. Springholz, V. Holy, M. Pinczolits, and G. Bauer, *Science* **282**, 734 (1998).
- <sup>24</sup>K. Akahane, N. Ohtani, Y. Okada, and M. Kawabe, *J. Cryst. Growth* **245**, 31 (2002).
- <sup>25</sup>R. Oshima, T. Hashimoto, H. Shigekawa, and Y. Okada, *J. Appl. Phys.* **100**, 083110 (2006).
- <sup>26</sup>P. B. Joyce, T. J. Krzyzewski, P. H. Steans, G. R. Bell, J. H. Neave, and T. S. Jones, *J. Cryst. Growth* **244**, 39 (2002).
- <sup>27</sup>Y. Bessho, Y. Harada, T. Kita, E. Taguchi, and H. Yasuda (to be published).
- <sup>28</sup>P. Yu, W. Langbein, K. Leosson, J. M. Hvam, N. N. Ledentsov, D. Bimberg, V. M. Ustinov, A. Yu. Egorov, A. E. Zhukov, A. F. Tsatsul'nikov, and Yu. G. Musikhin, *Phys. Rev. B* **60**, 16680 (1999).
- <sup>29</sup>E. C. Le Ru, A. J. Bennett, C. Roberts, and R. Murray, *J. Appl. Phys.* **91**, 1365 (2002).
- <sup>30</sup>A. Polimeni, A. Patane, M. Henini, L. Eaves, and P. C. Main, *Phys. Rev. B* **59**, 5064 (1999).
- <sup>31</sup>T. Sugaya, T. Amano, M. Mori, and S. Niki, *Appl. Phys. Lett.* **97**, 043112 (2010).
- <sup>32</sup>J. Bellessa, V. Voliotis, R. Grousson, X. L. Wang, M. Ogura, and H. Matsuhata, *Phys. Rev. B* **58**, 9933 (1998).
- <sup>33</sup>H. Fu, L.-W. Wang, and A. Zunger, *Phys. Rev. B* **59**, 5568 (1999).
- <sup>34</sup>H. Akiyama, S. Koshiba, T. Someya, K. Wada, H. Noge, Y. Nakamura, T. Inoshita, A. Shimizu, and H. Sakaki, *Phys. Rev. Lett.* **72**, 924 (1994).
- <sup>35</sup>D. Gershoni, M. Katz, W. Wegscheider, L. N. Pfeiffer, R. A. Logan, and K. West, *Phys. Rev. B* **50**, 8930 (1994).
- <sup>36</sup>D. S. Citrin, *Phys. Rev. Lett.* **69**, 3393 (1992).
- <sup>37</sup>A. Feltrin, J. L. Staehli, B. Deveaud, and V. Savona, *Phys. Rev. B* **69**, 233309 (2004).
- <sup>38</sup>M. Sugawara, K. Mukai, Y. Nakata, H. Ishikawa, and A. Sakamoto, *Phys. Rev. B* **61**, 7595 (2000).
- <sup>39</sup>P. Borri, W. Langbein, S. Schneider, U. Woggon, R. L. Sellin, D. Ouyang, and D. Bimberg, *Phys. Rev. Lett.* **87**, 157401 (2001).